Biophysical Chemistry 28 (1987) 253–263
Elsevier

BPC 01204

The charge effects of the self-diffusion constant of bovine mercaptalbumin

Fumiko Hirakawa [a], Shigeo Yoshino [a], Seiichi Era [b], Kazuo Kuwata [b], Masaru Sogami [b] and Nobuhisa Imai [a]

[a] *Department of Physics, Faculty of Science, Nagoya University, Nagoya 464 and* [b] *Department of Physiology, Medical School, Gifu University, Gi'u 500, Japan*

Received 9 December 1986
Revised manuscript received 13 October 1987
Accepted 14 October 1987

Diffusion constant; Dynamic light scattering; Albumin; Charge effect; Polyelectrolyte

The charge effect on the translational self-diffusion constant, D, of polyelectrolytes has been quantitatively analyzed based on dynamic light scattering experiments. Perfectly monodisperse bovine mercaptalbumin has been used at low pH as a positively charged polyelectrolyte sample. Completely linear plots of $\log\{g_2(t)-1\}$ vs. time t have been obtained for uncharged states of the protein, for the correlation function of the scattered light intensity, $g_2(t)$. The plots deviate from linearity as polyions bear the charges. The D values for various ionic states, obtained from the initial slopes of the plots, have been analyzed using the simple theory of Imai and Mandel (N. Imai and M. Mandel, Macromolecules 15 (1982) 1562) derived based on the Onsager-Navier-Stokes equation for solvent flow with counterion distribution around a polyion. It has turned out that the experimental D values coincide well with the theory and that the characteristic nature of D can be elucidated principally from the charge effect.

1. Introduction

The purpose of this paper is to clarify the charge effects on classical self-diffusion constants of polyions in solution. For this purpose, in this study, the experimental self-diffusion constant, D, is obtained for bovine mercaptalbumin (BMA) under various ionic conditions from dynamic light scattering measurements under the consideration of reasonable correlation time scales. These D values are analyzed by examining whether the behavior of D, especially the dependence on polyion concentration, C_p, or salt concentration, C_s, coincides with the theoretical expression. Generally, as indicated by the theories, the diffusion of polyions displays a nonlinear character with respect to C_p, and its dependence on C_s or polyion charge z is also quite complicated. It is, therefore, meaningful to determine to what extent the theoretical expressions can elucidate the behavior of experimentally obtained D values.

Raj and Flygare [1] have dealt with a similar problem based on dynamic light scattering measurements on bovine serum albumin. They interpreted their data on D, showing a nonlinearity with respect to polyion concentration C_p, as being due to the polyion-polyion interaction and the C_p-dependent friction constant. The C_p and C_s ranges in their measurements, however, were limited for quite concentrated states. They have shown that in such a state D is approximately expressed as a linear function of C_p. However, since our present purpose is to determine the validity of polyelectrolyte theories, it is necessary to extend both concentrations to more dilute ranges.

In recent studies of diffusion phenomena of charged macromolecules, one of the most important problems which require clarification is

Correspondence address: F. Hirakawa, Department of Physics, Faculty of Science, Nagoya University, Nagoya 464, Japan

obviously the basic nature of the time dependence of diffusion constants, since the diffusion process generally comprises many time components corresponding to the complicated interaction mechanisms involved in solution, such as polyion-polyion or polyion-counterion interactions. The time resolution of D has been theoretically formulated by Schurr [2] based on a coupled-mode theory. This study has clarified various important dynamic characteristics of polyelectrolytes; the concept of the relaxation time, τ_B, introduced in his theory is essential for describing the time resolution of D in such ionic systems having many relaxation mechanisms due to the coexistence of at least two sorts of interacting particles of extremely different sizes.

In studying polyion diffusion, however, not only these time-resolution problems, but also those concerning clarification of the electrolytic natures of classical self-diffusion based on thermodynamical polyelectrolyte theories are believed to be very important, since it remains to be elucidated whether the experimental D values principally obey the hydrodynamical or thermodynamical theories of polyelectrolytes.

The theoretical expressions for D have been obtained based on the equilibrium theories of polyelectrolytes proposed by Eisenberg [3], Alexandrowicz and Daniel [4] and Varoqui and Schmitt [5]. The essential part of this classical expression for D has also been derived as a special case by Schurr [2] on the basis of coupled-mode theory. However, the starting point of these theories (except Schurr's approach) rests on the simultaneous construction of two kinds of diffusion equations for polyions and small ions. This point of view is established under the assumption that both kinds of ions can be described simultaneously by equations of the same category with almost identical time scales of motions. This assumption is incorrect because of the extremely different particle sizes and relaxation times involved. Also, there is no guarantee that the expression for total force on a polyion is given by the well-known Stokes equation for hydrodynamic resistance plus electrostatic force separately calculated, since the Stokes equation has been derived only under the condition of the absence of a bulk force (like electrostatic force) on the solvent.

To solve such problems in classical polyion diffusion, a more rational derivation of the expression for D has been recently presented by Imai and Mandel [6] based on a combination of the Onsager-Navier-Stokes hydrodynamic equation and polyelectrolyte theories. This theory calculates the force acting on the solvent flow relative to a polyion, instead of the forces on solute ions. This theory also distinguishes the difference in relaxation times between polyions and small ions by introducing the concept of a cell model. We adopted this theory for our present purposes, since this theory has some merits in comparison with the experimental results; for instance, the concept of apparent polyion charge, which is experimentally significant, automatically appears in this theory in the derivation as a difference between the concentration and activity of counterions. Although the cell model itself may not be theoretically ideal, it is rational as a first step toward evaluation of the effect of a strong polyion-counterion interaction in fundamental polyion diffusion, since the relaxation time for the migration processes of polyions (which probably could be expressed by Schurr's τ_B [2]) is sufficiently long compared to that of the free part of low molecular weight ions around the polyion.

Now, in order to determine the charge effect of polyions from experimental plots of $\ln\{g_2(t)-1\}$ vs. t in dynamic light scattering measurements, where $g_2(t)$ is the correlation function and t the time, it is necessary to establish first whether these plots for uncharged states are linear with a slope corresponding to the theoretical value of $D = kT/6\pi\eta a$ on the predicted time scale, where kT is the Boltzmann factor and a the protein radius in a solvent of viscosity η. As shown in section 2, it turns out in our experiments that these conditions are fully satisfied for uncharged states taking place at $C_s \to \infty$ or at the isoelectric points.

For charged states, as shown by our results, it is found that the plots deviate remarkably from linearity as proteins bear the charges. It is reasonable to assume that the classical D values can be obtained from the initial slopes of the corresponding $\ln\{g_2(t)-1\}$ vs. t plots even for charged states of the proteins.

Through analyses of our experimental results, it has been concluded that the behavior of D thus determined can be well elucidated by the theory as being due to protein charge effects. However, it remains a problem requiring elucidation in the future to explain the cause of the above deviation of $\ln\{g_2(t)-1\}$ vs. t plots from linearity, in relation to charge effects. In order to develop this problem, it is necessary to introduce a coupled-mode theory as has been developed by Schurr [2].

2. Materials and methods

2.1. Materials

Crude crystallized bovine plasma albumin (BPA) purchased from Armour Pharmaceutical Co. was used after the following purification. It was first defatted according to a modification of Chen's charcoal-defatting method and filtered through a Triton X-100-free Millipore membrane (0.45 μm). Next, BPA was fractionated into bovine mercaptalbumin (BMA) by means of gel filtration on SE-Sephadex C-50 as described by Hagenmaier and Foster [7]. Finally, purified BMA was obtained by dialysis against deionized water for about 10 days in a cellophane tube. This BMA (molecular weight 66000) was identified by high-pressure liquid chromatography (HPLC) as being completely monodisperse, and the SH group of Cys^{34} in this BMA was almost undecorated.

2.2. Determination of total charge number on BMA

Buffer was not used in any of our experiments. The range of the initial pH after dialysis was between pH 5.0 and 5.4, close to the isoelectric point (pH 5.2). The process of inducing a charge on this protein (to a positive sign) was performed by means of the addition of HCl. Since the pH in this study was limited to below pH 5.2, CO_2 gas effects from the air could be completely avoided.

The BMA concentration was determined spectrophotometrically using an extinction coefficient of $\epsilon^{1\%}_{1\,cm} = 6.67$ (at 279 nm).

The total number of protein charges in solution was obtained by means of pH measurements. It is known that BMA consists of 582 amino acids, in which 99 are positively ionizable and 98 negatively. The number of charged amino acids in the pH range used in this study is listed in table 1.

Table 1

Number of ionizable amino acid groups and their pK' values in albumin

	Group	Number of amino acids	
		(n) [a]	pK' [b] (single component, at 25 °C)
Minus	Asp	39	3.86
	Glu	59	4.25
Plus	His	17	6.0
	Lys	59	10.53
	Arg	23	12.48

[a] Ref. 16.
[b] Ref. 17.

The sum of protein charges, z, was obtained experimentally from pH measurements by use of the following relation:

$$C_p z = \gamma_H C_H - a_H + 10^{-5.2} \quad (1)$$

where C_p and C_H are the respective molar concentration of protein and added HCl, needed to bring the solution to the present pH from the isoelectric point (pH 5.2), γ_H the activity coefficient of H^+ in a simple salt solution of the same concentration, and a_H the H^+ activity. Eq. 1 is established under the assumption that the number of bound H^+ (per protein) resulting from the H^+ added below the isoelectric point, which is expressed by eq. 1 completely adheres to the protein in the form of COOH. This assumption is very reasonable, since there is no H^+ atmosphere around the protein in its positively charged state. In this respect, γ_H can be regarded as equal to unity in the salt concentration range in our experiments, since $\gamma_H > 0.95$ for our pH range according to the table of Harned and Owen [8].

The pH measurements were made using a Radiometer pHM64-type pH meter. The titration cell was immersed in an isothermal water bath (25 ± 0.05 °C), the electrodes used being a Radiometer glass electrode (202C) and a saturated KCl-calomel reference electrode. Each H^+ titration was per-

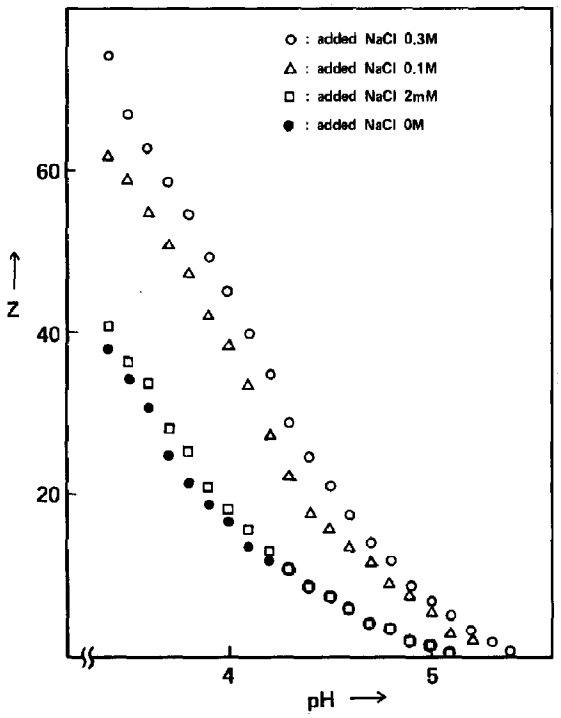

Fig. 1. Plots of charge on BMA vs. pH at various concentrations of added NaCl. BMA concentration: 0.2%.

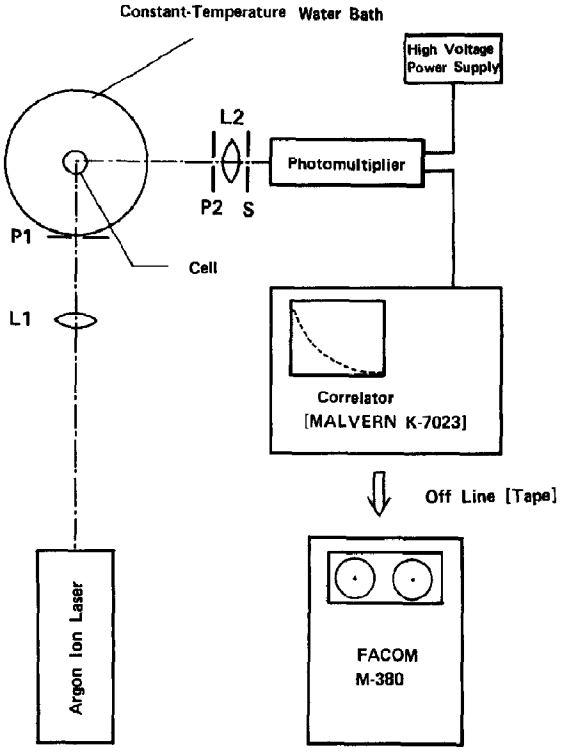

Fig. 2. Block diagram of the apparatus used in dynamic light scattering measurements.

formed by successive additions of HCl from a micrometer syringe (Gilmont, S-1100) (total capacity, 0.2 ml; smallest scale division, 0.1 μl) to the protein solution (~ 5 ml).

For example, z obtained from eq. 1 is shown in fig. 1 as a function of pH at various NaCl concentrations. The titration curve for 0.1 M salt coincided well with the data of Sogami and Foster [9]. (There is no published report concerning the z vs. pH relation for other salt concentrations.)

2.3. Measurement of diffusion constant D

A homodyne method was applied to our dynamic light scattering measurements. The optical system is depicted schematically in fig. 2. Monochromatic light from an argon ion laser (Spectra Physics 165, wavelength 488 nm) was focussed onto the cell by means of the lens L1 and pinhole P1. The scattered light was focussed onto a photomultiplier on the turntable after passing through pinhole P2, lens L2 and then the slit S. The intensity correlation of the scattered light was obtained by using a Malvern correlator (system K-7023), and the analyses were performed with a Facom M-380 computer. The scattering cell was placed in an isothermal water bath at 25.0 ± 0.2 °C.

The scattering angle θ was always kept constant at 90° for convenience, since in several trial cases, it was found that $1/\tau$ (reciprocal of the relaxation time $1/q^2D$, where q is the scattering vector) was perfectly linear with respect to $\sin^2(\theta/2)$.

3. Results

3.1. Importance of monodispersity

A perfectly linear relation can be expected between $\log\{g_2(t)-1\}$ and t only if the following

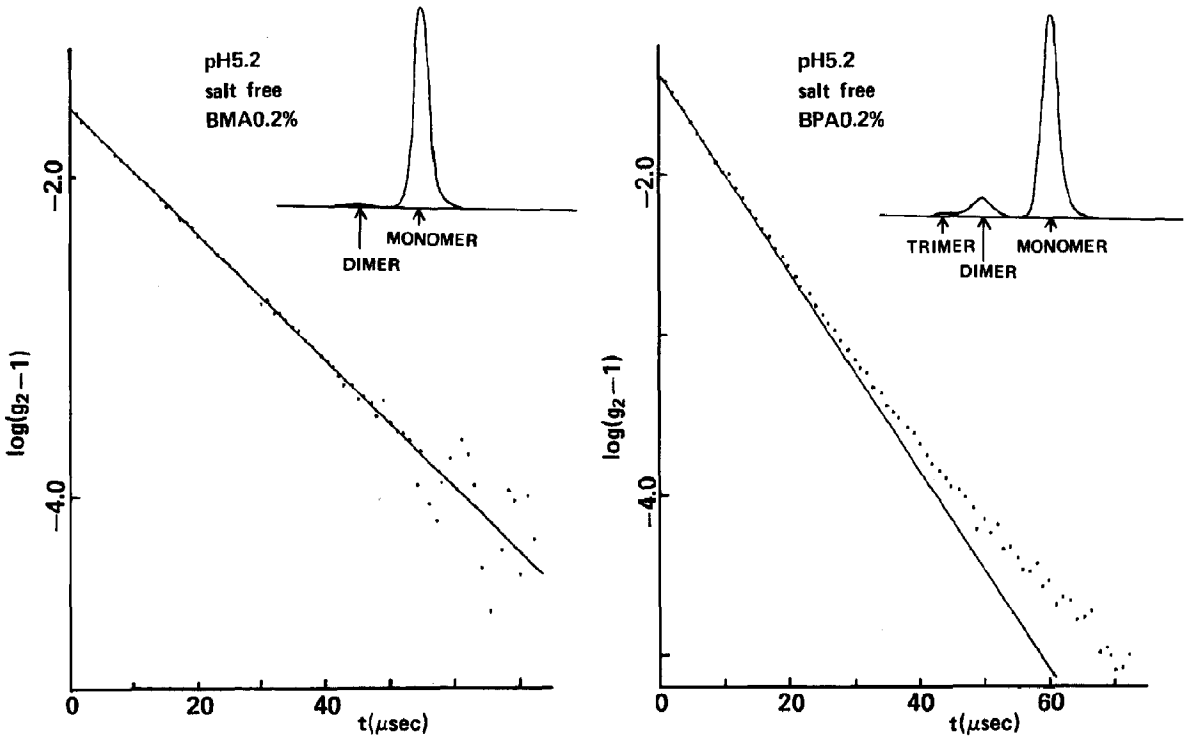

Fig. 3. Plots of $\log\{g_2(t)-1\}$ vs. t for BMA (left) and BPA (right). The inset in each figure shows the data obtained from HPLC.

conditions are satisfied: (A) particles are spherical, (B) particles are monodisperse, and (C) mutual interactions between particles can be ignored. The BPA solutions which have been ordinarily used never show any single-relaxation pattern even in the uncharged states owing to the presence of contamination (mainly by the dimer forms). Since our aim is only to detect the charge effects on D, perfect monodispersity of the sample is of great necessity.

The features of monodispersity of BMA (purified) and BPA (unpurified) as measured by HPLC are shown in the left- and right-hand panels of fig. 3, respectively. The corresponding dynamic light scattering data are also indicated in this figure. Fig. 3 clearly demonstrates the importance of monodispersity. It should be emphasized that in the case of unpurified samples, the D values obtained from the initial slope always vary irregularly depending on the degree of polydispersity.

3.2. pH dependence of D as a function of added NaCl

Fig. 4 shows the entire manner of the pH dependence of D under various ionic conditions at a fixed concentration of BMA (0.09%).

We selected a much lower range of protein concentrations than that in ref. 1 to avoid the influence of mutual protein interactions, although the dynamic light scattering measurements required higher sensitivity.

In fig. 4, the filled and semi-filled symbols represent the data when $\log\{g_2(t)-1\}$ is completely linear vs. time t, linearity being maintained beyond the point corresponding to twice the relaxation time, 2τ. The unfilled symbols represent those plots which deviate from linearity in spite of being obtained on monodisperse systems. The characteristics of these deviations are shown in detail in fig. 5. The deviations are undoubtedly due to the charge effect.

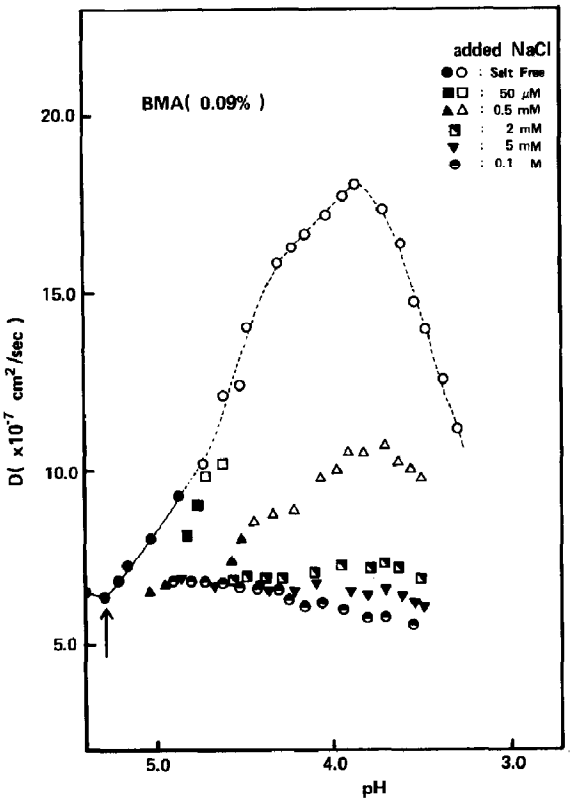

Fig. 4. Diffusion constant, D, as a function of pH at various concentrations of added NaCl.

If the protein solution is near the isoelectric point, the protein must exhibit a similar behavior to neutral polymers, so that in this case one can compute the protein radius from the experimental D value based on the Einstein-Stokes equation. The radius obtained was 38 Å in salt-free solution, in accordance with the result obtained from a fluorescence-rotation experiment [10].

It is known from the viscosity data of Tanford et al. [11] and the small-angle light scattering results obtained by Muroga et al. [12] that the radius becomes larger as the pH decreases below the isoelectric point even for high salt concentrations. Our data (shown in fig. 6) give almost the same results as those of Tanford et al. The same tendency toward protein expansion resulting from a pH decrease is also clearly shown in the data of Muroga et al., although their conclusion is based on the data obtained at only three pH values. It is possible that this change in radius is due to an electrolytic frictional effect.

Now, let us assume that the translational diffusion constant for the uncharged state at a given pH, D_0, is given by D at 0.1 M salt concentration, then the charge effect can be analyzed from the differences between D and D_0.

As shown in fig. 4, the D values increase sharply as the pH decreases for low salt concentrations, and after attaining the maximum at pH 3.8 begin to decrease. As described quantitatively in section 3.4, this decrease in D can be attributed to the increase in Cl^- concentration resulting from HCl addition which screens the net protein charges.

3.3. Relation between appurent polyion charge and pH

When the pH of a solution is acidic, the total number of H^+ in the solution including those in the form of COOH remains constant despite the addition of neutral salt, since no H_2O is formed. Let us define the free energy change, δF, in the process of H^+ transfer from a place far from the polyion to the vicinity of a COO^- group on the polyion. If the electrostatic potential around a COO^- group is given by ψ_p, and the short-range interaction between a COO^- group and H^+ when forming a COOH group is denoted by χ_H, δF is expressed by the equation:

$$\delta F = -kT \ln a_H + e_0\psi_p + \chi_H - kT \ln v_H \qquad (2)$$

where v_H represents the volume of the region in which H^+ becomes entrapped in the vicinity of COO^- in the process of COOH formation. We assume that χ_H and v_H are constants unaffected by electrolytic circumstances with the consideration that each quantity must take an intrinsic value in the COOH-forming state. In the equilibrium state, since δF in the above expression should be zero, we have the relation

$$e_0\psi_p = kT \ln a_H - \chi_H + kT \ln v_H$$
$$= kT \ln a_H + \text{constant} \qquad (3)$$

The relationship expressed by eq. 3 is subject to the above-mentioned assumptions, i.e., χ_H = constant and v_H = constant.

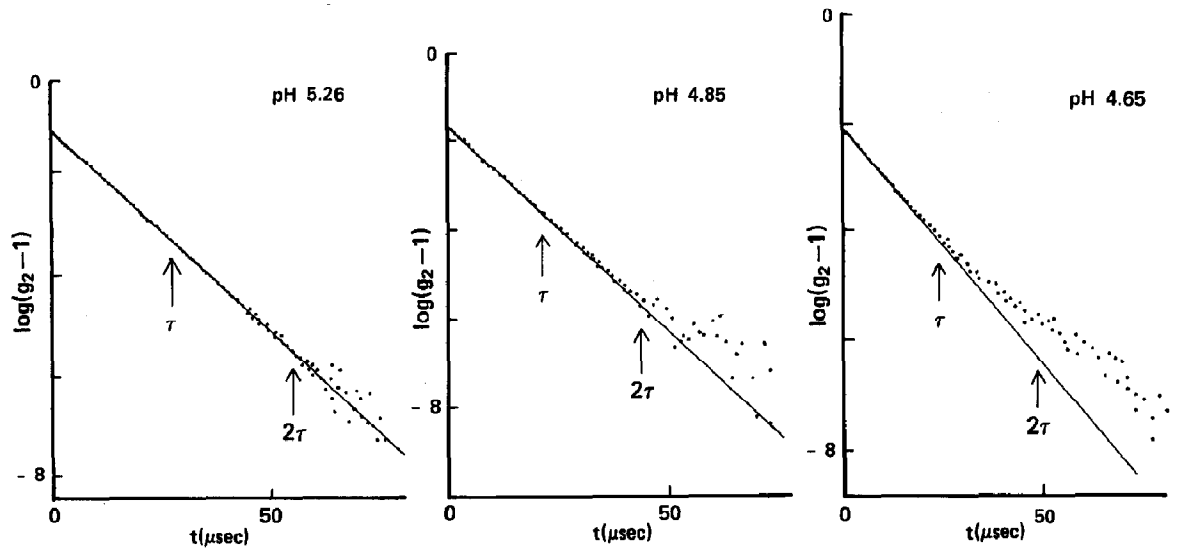

Fig. 5. Plots of $\log\{g_2(t)-1\}$ vs. t for BMA in salt-free solution. Arrows indicate relaxation time τ or 2τ. Protein concentration, 0.27%. Deviation from linearity in the charged states is clearly demonstrated.

It should be emphasized that eq. 3 is valid only when the pH of the solution is acidic; when the range of pH is above pH 7.0, the free energy of formation of H_2O should be introduced into δF, since some fraction of H^+ is converted to H_2O in the above-mentioned hypothetical transfer.

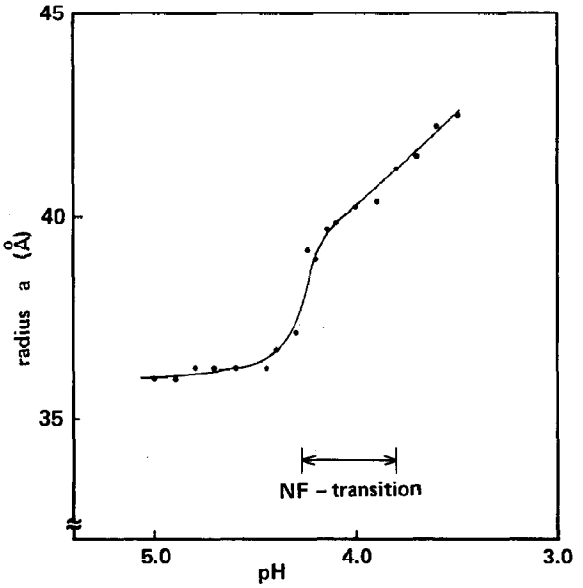

Fig. 6. Radius of BMA as a function of pH, obtained from the data at 0.1 M NaCl.

On the other hand, since ψ_p is believed to be a function only of the apparent polyion charge z^* on a given polyion, the above equation shows that z^* is a function of pH alone, i.e.

$$z^* = f(\mathrm{pH}) \tag{4}$$

This means that if the pH of the solution is fixed, then z^* should remain almost constant on addition of neutral salt. It should be noted that the parameter ψ_p above is the electrostatic potential just near a COO^- group. The difference between this ψ_p and the potential obtained by titration will be discussed theoretically elsewhere.

In our present work, we attempted to analyze the experimental data by assuming temporarily that eqs. 3 and 4 hold. As described in section 3.4, we have obtained reasonable results from analyses based on these relations.

3.4. Dependence of D on C_p and C_s at fixed pH values

The behavior of D at pH 3.8 is depicted in fig. 7 as a function of BMA concentration C_p (on a molarity scale) at salt concentrations $C_s = 0.16$, 0.21, 0.26, 0.31, 0.71 and 2.16 mM. The definition

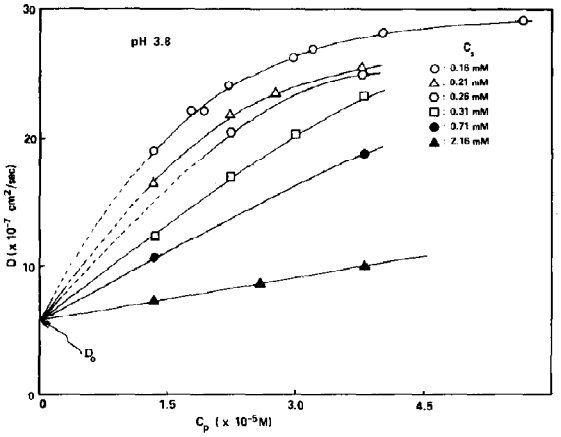

Fig. 7. Plots of D vs. C_p at a fixed pH of 3.8.

of C_s is given by;

$$C_s = a_H + C_{Na}$$

or

$$C_s = [Cl^-]_{total} - zC_p \tag{5}$$

where $[Cl^-]_{total}$ is the concentration of Cl^- (counterion) from added HCl and NaCl, and z the charge number of a BMA molecule; zC_p being the total charge on BMA molecules per l.

As demonstrated in fig. 7, plots of D at C_s above 0.31 mM converge linearly to D_0 when extrapolating C_p to zero at a fixed pH. Even for C_s below 0.31 mM, this D_0 value is acceptable as the value of D extrapolated to $C_p = 0$. This tendency has also been investigated at other pH values, namely, pH 4.2, 4.0 and 3.6. It has also been found that this extrapolated value of D_0 coincides well with that of D separately measured at $C_s \to \infty$ (practically $C_s = 0.1$ M). It should be noted that even when C_s is moderately large and accordingly the charge effect is believed to be insignificant, D is still a linear function of C_p, i.e., the diffusion is of nonlinear character.

Let us attempt to clarify the behavior of D shown in fig. 7 assuming that the dependence of D on C_p or C_s is due mainly to the polyion-counterion interaction. This effect has been dealt with theoretically by Varoqi and Schmitt [5] and Eisenberg [3], and more strictly by Imai and Mandel [6]. According to the theory [6], D is expressed by following equation,

$$D = \frac{kT}{\xi_p}\left[\phi_p + \frac{(z\gamma_p)^2 C_p\{1-(\xi_s/\xi_p)\}}{(2C_s + \gamma_p z C_p) + (\xi_s/\xi_p)(z\gamma_p)^2 C_p}\right] \tag{6}$$

where ξ_p is the frictional constant of an uncharged polymer, ξ_s the averaged frictional constant of small ions, γ_p the degree of shielding of net polyion charges by counterions, z the number of polyion charges, and ϕ_p the osmotic coefficient of the polyion solution. The quantity $z\gamma_p$ represents the effective polyion charge, which may be regarded as z^*. The quantity, ϕ_p, in the first term represents the contribution of the polyion-polyion interaction, the second being due to the polyion-counterion interaction. The theory of Imai and Mandel [6] has proved that the effective polyion charge in diffusion processes is expressed solely by the thermodynamic quantity $z\gamma_p$.

We now consider the experimental data based on eq. 6 under the assumption $\phi_p \to 1$. This assumption should be valid provided that C_s is not extremely low and C_p not excessively high.

The significant characteristics of D predicted from eq. 6 are summarized as follows:

(A) D should be a unique function of C_p/C_s, for a fixed z^*.

(B) In the region where the condition $C_p/C_s \ll [2/z^*\{1+(\xi_s/\xi_p)z^*\}]$ is established, D should be approximately expressed by

$$D = \frac{kT}{\xi_p}\left\{1 + \tfrac{1}{2}z^{*2}\left(1 - \frac{\xi_s}{\xi_p}\right)\frac{C_p}{C_s}\right\} \tag{7}$$

This equation shows a linear increase of D vs. C_p/C_s when z^* is fixed.

(C) The quantity $D_0/(D-D_0)$, in which D_0 is the diffusion constant of uncharged polymers expressed by $D_0 = kT/\xi_p$, is a linear function of C_s/C_p throughout the range of C_s/C_p as given by the following equation;

$$\left(1 - \frac{\xi_s}{\xi_p}\right)\frac{D_0}{D-D_0} = \frac{1+(\xi_s/\xi_p)z^*}{z^*} + \frac{2}{z^{*2}}\frac{C_s}{C_p} \tag{8}$$

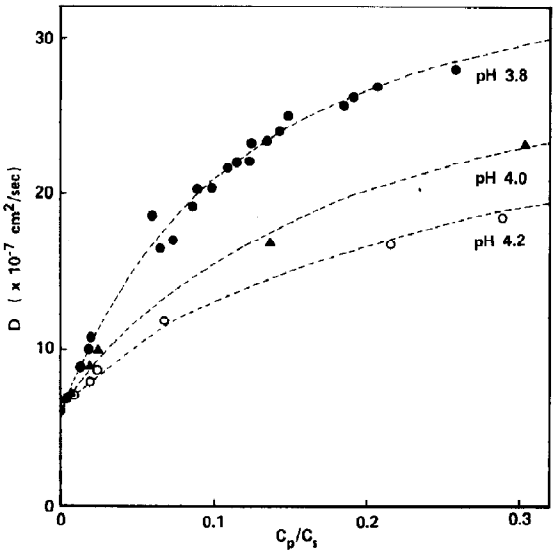

Fig. 8. Plots of D vs. C_p/C_s at pH 3.8, 4.0 and 4.2. (------) Theoretical curves based on eq. 6 and table 2.

Now, according to eq. 6, it would be a good test of the validity of the theory to determine whether the experimental D in fig. 7 is a unique function of C_p/C_s at a fixed value z^* i.e., at a fixed pH referring to eq. 4. The results of such a test are shown in fig. 8. It is found that all the plots, D vs. C_p/C_s, lie on one curve at a fixed pH, which thus implies the validity of the theory. Also, the prediction from the theory that the values of D must increase linearly with C_p/C_s when C_p/C_s satisfies the relation;

$$\frac{C_p}{C_s} \ll \frac{2}{z^*\left\{1+\left(\xi_s/\xi_p\right)z^*\right\}}$$

is also examined in fig. 9.

Table 2

Apparent charge on BMA, z^*, and ratio of the frictional constant of a counterion to that of the protein, ξ_s/ξ_p

pH	z^*	ξ_s/ξ_p
4.2	5.5	0.055
4.0	7.1	0.065
3.8	10.0	0.060
3.7	10.3	0.054
3.6	10.6	0.056
3.5	11.0	0.068

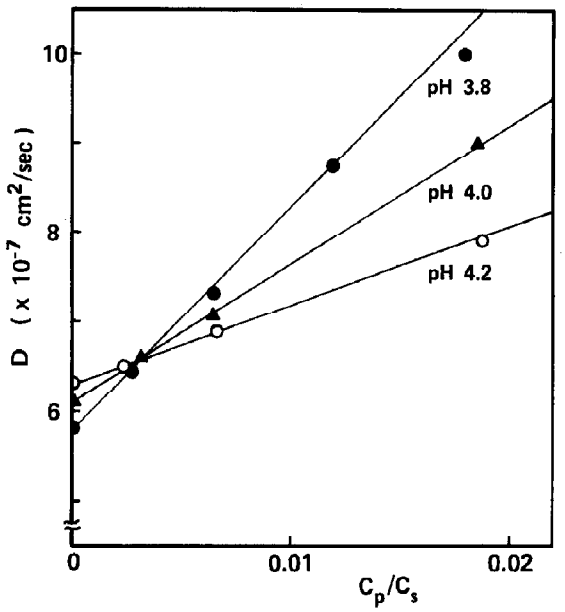

Fig. 9. Same data as in fig. 8 near $C_p/C_s = 0$ on an expanded scale. The differences in D values seen at $C_p/C_s = 0$ are due to differences in protein radius.

On the other hand, experimental examination of eq. 8 is also important, i.e., whether the quantity $D/(D - D_0)$ is proportional to C_s/C_p over the

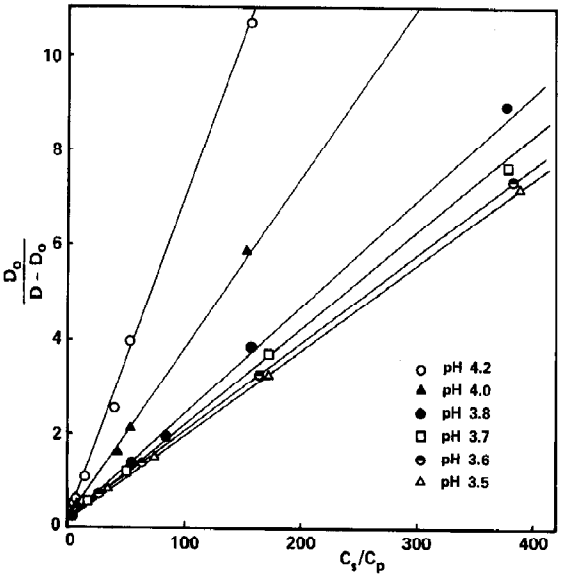

Fig. 10. Plots of $D_0/(D - D_0)$ as a function of C_s/C_p at pH 4.2, 4.0, 3.8, 3.7, 3.6 and 3.5.

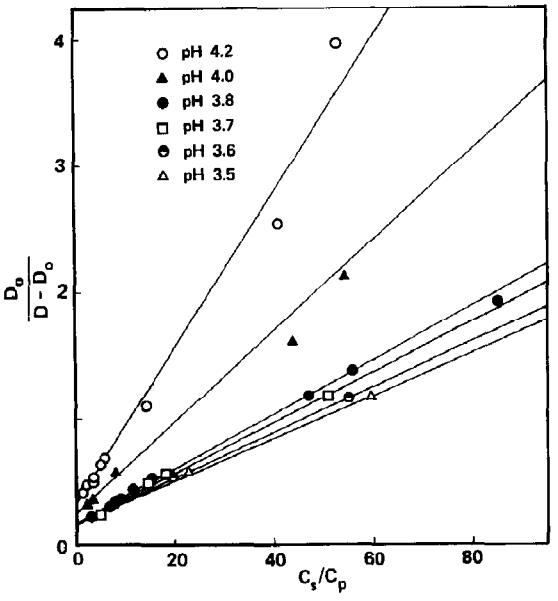

Fig. 11. Same data as in fig. 10 around $C_s/C_p = 0$ on an expanded scale.

entire range of C_s/C_p provides stricter confirmation of the validity of eq. 6. As depicted in fig. 10, it is found that eq. 8 is experimentally established over a wide range of C_s/C_p. Fig.11 illustrates the same results on an expanded scale around small C_s/C_p values. The intercept in fig. 11 gives the quantity, A, at each pH value, and the slopes in figs. 10 and 11, lead to the quantity B at various pH values;

$$A = \frac{1 + (\xi_s/\xi_p)z^*}{z^*\{1 - (\xi_s/\xi_p)\}}, \quad B = \frac{2}{z^{*2}\{1 - (\xi_s/\xi_p)\}} \tag{9}$$

By eliminating ξ_s/ξ_p in A and B one can obtain the value of z^* from the relation;

$$z^{*2} + z^* - 2(1 + A)/B = 0 \tag{10}$$

The z^* values are listed in table 2 at various pH values, together with the numerical values of ξ_s/ξ_p.

The values of γ_p $(= z^*/z)$ can be obtained as a function of C_s at various fixed z values as indicated in fig. 12. The theoretical D values using the numerical values of z^* and ξ_s/ξ_p above are indicated by dotted lines in fig. 8 for the entire range of C_p/C_s at various fixed pH values.

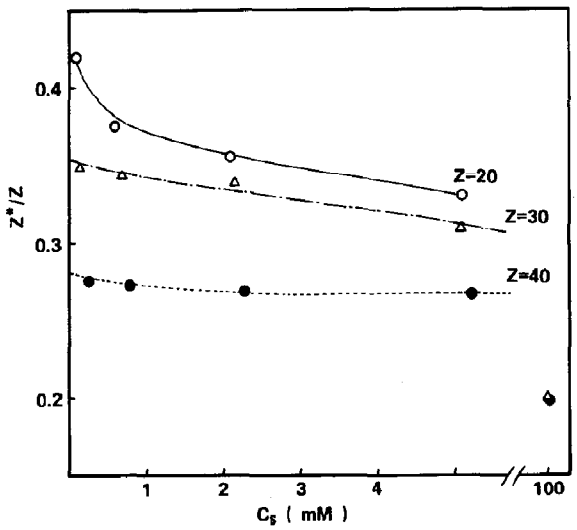

Fig. 12. Plots of the shielding factor, γ_p $(= z^*/z)$ vs. C_s at various fixed values of z.

4. Discussion

It is noteworthy that in the pH range below the isoelectric point, the protein charge z obtained from eq. 1 is believed to be more accurate than that based on the usual method of salt-blank subtraction, since H^+ is not a counterion but a coion, whose activity coefficient is almost exactly unity as investigated in polyelectrolyte theories.

It should also be noted that, as mentioned in section 3.3, we have analyzed the data using eq. 6, or the equivalent expressions, eqs. 7 and 8, under the assumption that eq. 4 is valid. The fact that the plots of D on the same pH line are expressed by a unique function of C_p/C_s shows that eq. 4 is very reasonable in our present systems, where the pH is lower than 4.2.

It is rather surprising that the experimental results could be almost perfectly explained by the theory including the effect of the ξ_s/ξ_p term, in spite of the above multi-extrapolation analyses, such as the findings of the tangents in fig. 5 and the slopes and intercepts in fig. 10 and 11.

The numerical value obtained for the parameter ξ_s/ξ_p (≈ 0.06) is also reasonable under the consideration that ξ_s/ξ_p is expressed by the ratio of the

radius of a small ion to that of a protein, the former being 2 Å in the hydrated state and the latter 40 Å. However, the fact that the protein radius has a tendency to increase with decreasing pH, as described in section 3.2, is not very evident in the present experimental values of ξ_s/ξ_p. This test is too severe in the above extrapolation processes.

The relation between γ_p $(=z^*/z)$ and C_s at various fixed z values obtained from the above analyses is illustrated in fig. 12. This graph also shows that despite the above-described multiple plotting analysis the γ_p obtained is in reasonably satisfactory agreement.

It is still a difficult problem to explain the deviation of $\ln\{g_2(t)-1\}$ vs. t plots from linearity occurring at large t even in purified monodisperse albumin solutions. This shift is no doubt due to an electrostatic effect, since no such phenomenon was observed for uncharged states of pure albumin as depicted in the left-most panel in fig. 5. Qualitatively speaking, this shift is thought to be due to a multi-relaxation process of counterions resulting from the wide spread distribution of their concentration around a polyion. Such a multi-relaxation process may be the same as that detected in dielectric experiments. It would be desirable to develop the theory to account for this problem in the line of the study of Stephen [13] under the consideration of nonlinear characteristics for the counterion distribution. As another explanation it is possible that this effect is due to the OE transition which has been pointed out by Schurr and Schmitz [14], and Drifford and Dalbiez [15].

From the various results described above, it may be concluded that the remarkable nature of the diffusion of albumin found in our dynamic light scattering measurements could be reasonably explained in terms of the electrostatic interaction between a polyion and its counterions.

Acknowledgements

The authors wish to express their thanks to their laboratory members, Drs H. Suda, S. Matsuura and S. Tsurumi, for making valuable suggestions. The authors are also indebted to Dr. E. Suzuki, Medical School of Gifu University, for his considerable help in the purification work on BMA which required a skillful technique.

References

1 T. Raj and W.H. Flygare, Biochemistry 13 (1974) 3336.
2 J.M. Schurr, Chem. Phys. 111 (1987) 55.
3 H. Eisenberg, Biological macromolecules and polyelectrolytes in solution (Clarendon Press, Oxford, 1976).
4 Z. Alexandrowicz and E. Daniel, Biopolymers 1 (1963) 447.
5 R. Varoqui and A. Schmitt, Biopolymers 11 (1972) 1119.
6 N. Imai and M. Mandel, Macromolecules 15 (1982) 1562.
7 R.D. Hagenmaier and J.F. Foster, Biochemistry 10 (1971) 637.
8 H. Harned and B.B. Owen, The physical chemistry of electrolytic solution (Reihold, New York, 1958) p. 466.
9 M. Sogami and J.F. Foster, Biochemistry 7 (1968) 2172.
10 M. Sogami, K.D. Itoh and Y. Nemoto, Biochim. Biophys. Acta 393 (1975) 446.
11 C. Tanford, J. Buzzell, D. Rands and S. Swanson, J. Am. Chem. Soc. 77 (1955) 6421.
12 Y. Muroga, I. Noda, M. Nagasawa and T. Fukano, Biophys. Chem. 13 (1981) 97.
13 M.J. Stephen, J. Chem. Phys. 55 (1971) 3878.
14 J.M. Schurr and K.S. Schmitz, Annu. Rev. Phys. Chem. 37 (1986) 271.
15 M. Drifford and J.-P. Dalbiez, Biopolymers 24 (1985) 1501.
16 V.M. Rosenoer, M. Orsatz and M.A. Rothschild, Albumin structure, function and uses (Pergamon Press, New York, 1977).
17 A.L. Lehninger, Biochemistry (Worth, New York, 1970).